Journal of Power Sources 196 (2011) 2351–2359

Contents lists available at ScienceDirect

Journal of Power Sources

journal homepage: www.elsevier.com/locate/jpowsour

An innovative optimal power allocation strategy for fuel cell, battery and supercapacitor hybrid electric vehicle

Zhihong Yu[a,1], Donald Zinger[a], Anima Bose[b,*]

[a] Department of Electrical Engineering, Northern Illinois University, DeKalb, IL 60115, United States
[b] Institute of Sustainable Energy and Environment, Department of Chemical and Biomolecular Engineering, Ohio University, Athens, OH 45701, United States

ARTICLE INFO

Article history:
Received 17 July 2010
Received in revised form 6 September 2010
Accepted 20 September 2010
Available online 29 September 2010

Keywords:
Fuel cell
Hybrid electric vehicle
Battery
Supercapacitor
Energy management

ABSTRACT

An optimal design of a three-component hybrid fuel cell electric vehicle comprised of fuel cells, battery, and supercapacitors is presented. First, the benefits of using this hybrid combination are analyzed, and then the article describes an active power-flow control strategy from each energy source based on optimal control theory to meet the demand of different vehicle loads while optimizing total energy cost, battery life and other possible objectives at the same time. A cost function that minimizes the square error between the desired variable settings and the current sensed values is developed. A gain sequence developed compels the choice of power drawn from all devices to follow an optimal path, which makes trade-offs among different targets and minimizes the total energy spent. A new method is introduced to make the global optimization into a real-time based control. A model is also presented to simulate the individual energy storage systems and compare this invention to existing control strategies, the simulation results show that the total energy spent is well saved over the long driving cycles, also the fuel cell and batteries are kept operating in a healthy way.

1. Introduction

Due to the concerns about the depletion of gasoline and its adverse environmental impact, there has been a dramatic shift in strategy to utilize pollution free renewable energy sources in vehicles. Fuel cell electric vehicles (FCEV) hold tremendous promise in this regard to replace fossil fuel in the long run. Although the fuel cell itself can be considered as a power source with nearly unlimited energy (only limit to hydrogen tank size) and almost zero pollution, there are obstacles such as high cost per unit power, poor transient performance, and inability to allow bi-directional power flow that need to be overcome. While progress is being made in fuel cell technology, there is an immediate need for efficient design of hybridization of the vehicle power train. Benefits from such design include capturing regenerative braking energy, lowering cost per unit power, providing optimization possibility and mitigating the stress on the fuel cell stack by shifting some portion of dynamic power demand to a second power source thus improving fuel cell life and efficiency.

This article introduces an optimal design of an innovative hybrid power system in a FCEV. Based on physical limits of cost, mass, and volume as well as load change limits, a hybrid system that includes fuel cells, battery, and supercapacitor as energy sources is designed. The design is implemented to take full advantage of each source's capabilities. In doing so, an active power-flow control strategy from each energy source based on optimal control theory is proposed here. The innovative power allocation strategy allows optimized power flow between fuel cell and battery. A cost function is established that minimizes the squared error between the desired variable settings and current settings. The optimization uses the current battery state of charge (SOC), battery SOC at the end of the cycle, and average power flow as optimization parameters in the cost equation. Weights are placed on these values to optimize for specific goals such as controlling the battery SOC ripple or reduced variation in fuel cell power flow. By updating the coefficients on real time basis, fuel used is limited while maintaining both components in their better, if not best working range. By implementing this technique, a set of feedforward and feedback algorithms is designed, and updating method of the controller is also evaluated.

Considering all nonlinearities of the whole power system, the robust controller as well as another instantaneous controller for battery/supercapacitor hybrid is programmed. The additional controller uses a smaller size supercapacitor to assist the battery and make the battery stack work in an even better way. The paper has simulated the whole vehicle energy flow based on different driving

* Corresponding author at: Department of Chemical and Biomolecular Engineering, Ohio University, Athens, OH 45701, United States. Tel.: +1 740 597 3297; fax: +1 740 593 0873.
E-mail address: bosea@ohio.edu (A. Bose).
[1] Present address: Enova Systems, 1560 West 190th St, Torrance, CA 90501, United States.

0378-7753/$ – see front matter © 2010 Elsevier B.V. All rights reserved.
doi:10.1016/j.jpowsour.2010.09.057

cycles using Matlab-Simulink and its energy efficiency is compared to other existing control strategy for FCEV.

2. Background, theory and calculation

2.1. Fuel cell, battery, and supercapacitor hybrid system design

Almost all existing hybrid power systems of FCEV mainly composed of fuel cell/battery hybrid (F/B) [1–4] or fuel cell/supercapacitor hybrid (F/C) [5–10]. For example, Toyota has made a FCEV based on F/B hybrid using a nickel–metal hydride (NIMH) battery pack as a second energy source, and Honda has made another model based on F/C hybrid using supercapacitor cells as power buffers. It is expected that fuel cell/battery/supercapacitor (F/B/C) hybrid can result in superb system performance and energy efficiency. Research is only starting to look at the use of all of these components in a hybrid vehicle [11].

For an F/B hybrid, the fuel cell stack supplies the cruising power, while the battery has three main functions: driving the fuel cell auxiliaries, providing additional power required for acceleration, and receiving regenerative braking energy. The battery used here can be lead acid, NIMH batteries or lithium-ion batteries.

A DC–DC boost converter is required at the fuel cell side and another bi-directional DC–DC converter is necessary at the battery side [12,13]. A boost converter is typically used to boost-up the fuel cell voltage to a DC bus (typically 300–500 V for commercial motor drives), while a bi-directional DC–DC converter can be configured as an isolated buck, boost or buck-boost type, depending on the battery stack configuration [14–17]. If an AC motor is used, then a DC/AC inverter is needed at the DC bus side.

Some published works indicate that the fuel cell or the battery can be connected directly to the high voltage bus while the other energy storage device's output current is actively controlled via the DC converter [2,3], thus one of the two DC converters can be neglected, that help to reduce some design complicacy. However, Thounthong et al. [4] suggested that fast load demand will cause a high voltage drop at the fuel cell side, known as the fuel starvation phenomena. On the other hand, battery voltage is always known to vary depending on the specific load and can be deeply drained. Therefore, neither fuel cell nor the battery could be an ideal constant voltage source for providing required power alone. Furthermore, the motor drive efficiency and the exact load current limit are hard to estimate due to the varying DC voltage value; therefore, for analyzing the control strategy, it is assumed the inverter has a constant DC voltage at input. The addition of DC–DC converters is thus necessary for implementing this active power flow control strategy.

For F/C configuration, fuel cell serves as the main power source, while the supercapacitor bank replaces battery in F/B configuration. While a supercapacitor has high power density it does not have very high energy density and cannot act as a good energy buffer. Therefore, if the required peak power in a vehicle load is much larger than the fuel cell peak power for an extended time, a very large stack of supercapacitors would be required. This would add considerably to the cost.

Considering the advantages and disadvantages of the different power sources in the above discussion, a new power system with an innovative power allocation strategy is proposed that integrates all three components (fuel cell, battery and supercapacitor) together. A schematic of three power component system is shown in Fig. 1. All three converters are required here but are integrated into one global converter with individual controls. All three power system components are actively controlled.

A supercapacitor could have a SOC that varies widely without affecting its life and, therefore, can be considered a power buffer.

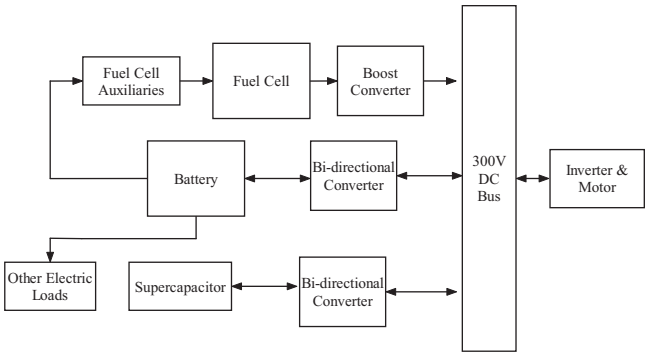

Fig. 1. Fuel cell, battery and supercapacitor hybrid vehicle power system configuration.

For this reason in the initial power flow optimization among the three energy storage devices the energy stored in the supercapacitor was neglected. Thus, the power system was divided into two parts, F/B hybrid and battery/supercapacitor (B/C) hybrid. In later part of the paper the F/B hybrid is proven to be able to minimize the energy cost while keeping battery working in a best SOC operating range. The B/C hybrid can provide a best power combination for any transient power request.

In this case, the new control system has integrated all merits of the F/B and F/C systems. Thus, the vehicle is possible to be optimized to obtain the longest lasting mileage and largest instant power with limits on cost, mass and volume.

2.2. Sizing of vehicle energy storage system

The vehicle platform for the FCEV used to exemplify this control system has characteristics in Table 1. The energy storage system is designed following a static optimization rule [18,19].

Considering the vehicle model in Table 1, for meeting energy and power requirements, we need to enforce the following equations:

$$W_T = \sigma_B M_B + \sigma_H M_H \geq 90\,\text{kWh} \tag{1}$$

$$P_T = \rho_B M_B + \rho_C M_C + \rho_{fc} M_{fc} \geq 80\,\text{kW} \tag{2}$$

$$P_C = \rho_B M_B + \rho_{fc} M_{fc} \geq 40\,\text{kW}. \tag{3}$$

We also need to minimize

$$V_T = V_B M_B + V_C M_C + V_{fc} M_{fc} + V_H M_H \tag{4}$$

$$C_T = C_B M_B + C_C M_C + C_{fc} M_{fc} + C_H M_H \tag{5}$$

$$M_T = M_B + M_C + M_{fc} + M_H, \tag{6}$$

where W_T is the total vehicle available energy; P_T is the peak total power; P_C is the cruising power; V_T is the total volume; C_T is the total cost; M_T is the total mass; σ_B and σ_H are the specific energy/kilogram for battery and hydrogen tank; ρ_B, ρ_C, and ρ_{fc} are the specific power/kilogram for battery, supercapacitor and fuel cell; V_B, V_C, V_{fc}, and V_H are the specific volume/kilogram for battery, supercapacitor, fuel cell and hydrogen tank; C_B, C_C, C_{fc}, and C_H are the specific cost/kilogram for battery, supercapacitor, fuel cell and hydrogen tank.

There are two directions available. One is try to specify the power and energy targets and minimize the cost, volume and weight. The other direction is to set an approximate maximum target for cost, volume, and weight, and try to maximize the power and energy. A mathematical programming method of such optimization has been introduced in Ref. [18,19]. The

Table 1
Fuel cell hybrid taurus 1990 characteristics.

Vehicle mass, m (kg)	1400	Drag coefficient, C_d	0.335
Frontal area, A (m^2)	2.47	Rolling resistance coefficient: f_r	0.01
Rolling radius, r_r (m)	0.3	Transmission gear ratio, N_t	3.21
Wheel mass, m_w (kg)	10	Final drive gear ratio, N_f	3.74
Wheel radius, r_w (m)	0.16	Transmission efficiency, η_t	0.92
Tire mass, m_t (kg)	10	Final drive gear efficiency, η_f	0.92
Tire radius, r_t (m)	0.22	Moment of inertia of a wheel/tire, $I_{w/t}$	1.224
Moment of inertia of motor and driveline $I_M N_f^2 N_f^2$	6.78	Air density, ρ_a	1.25
Motor efficiency, η_M	0.9		

Table 2
Vehicle energy storage systems design results.

NIMH battery mass (kg)	24.1	Hydrogen mass (without tank) (kg)	90
Supercapacitor mass (kg)	24	Fuel cell mass (kg)	217
Battery total energy (kWh)	1.33	Supercapacitor total energy (Wh)	96
Battery peak power (kW)	24.1	Supercapacitor peak power (kW)	84
Hydrogen total energy (kWh)	135	Fuel cell peak power (kW)	48
Vehicle energy (kWh)	136.3	Vehicle peak power (kW)	156
Energy system mass (kg)	355.1	Energy system cost ($)	8810
Energy system volume (L)	355.8	Traction motor	AC55

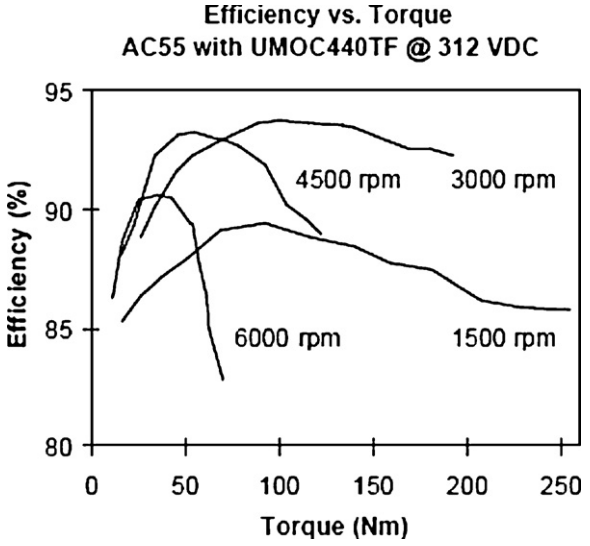

Fig. 2. AC55 motor efficiency.

resultant energy and power storage requirements are listed in Table 2.

To study the entire system, the drive motor needs to be characterized. The motor used in this study is the AC55. Its efficiency is provided in Fig. 2 [20].

2.3. Optimization of power allocation

There have been many articles published on dynamic power allocation of FCEV [7,21–23]. The most wildly acknowledged real-time control strategies are similar to those used in internal combustion engine (ICE) hybrid vehicles. These include charge depleting mode and charge sustaining mode control. There have been some global optimization strategies of energy management systems, such as dynamic programming or optimal control for ICE hybrid vehicles [23]. From control theory, for a stable optimal control system based on a vehicle platform, some future driving conditions must be provided by scheduled driving cycles [5,24]. Thus, typical optimal control techniques are not suitable for any real-time control. The difference between the proposed strategy and the aforementioned strategies will be discussed.

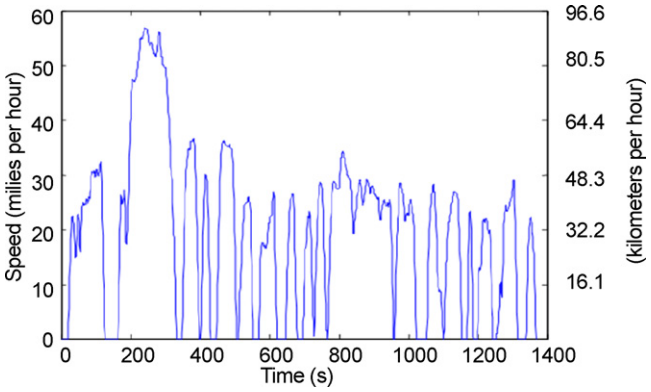

Fig. 3. UDDS, urban dynamometer driving schedule driving cycle.

For the proposed strategy two long driving cycles are evaluated; they are Urban Dynamometer Driving Schedule (UDDS, Fig. 3) and US06 highway portion (Fig. 4) [25]. Both cycles assume a flat road with no grade. The test will run each cycle for 5 h.

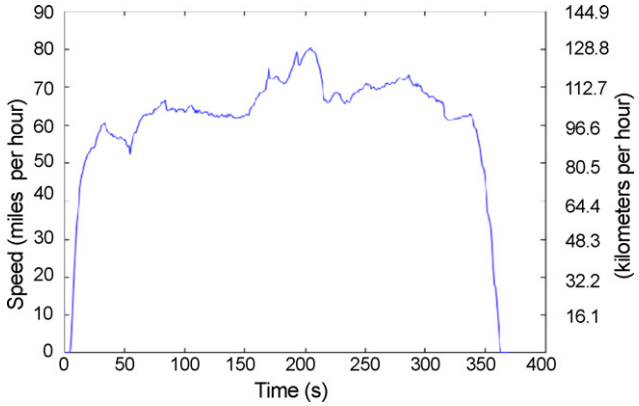

Fig. 4. US06 highway driving.

2.4. System model

In F/B hybrid system, the energy system to be controlled is described at the battery side,

$$x_{k+1} = x_k + (\eta_k u_k - \varphi_k)E_{ff} \tag{7}$$

where k is the time sample, x_k represents the state of the battery (which is the SOC times the maximum battery capacity), and η_k is the fuel cell converting efficiency for power flowing from the fuel cell to the power bus side. The efficiency can be different based on time-varying variables such as load change, temperature, etc. This efficiency is calculated from fuel cell output terminal voltage and current signals and is then compared with input power.

φ_k is a series of power requests depending on the driving cycle. It usually takes about 1–2 s for a fuel cell to respond to a power request based on latest technologies. Thus, a state change in the battery and fuel cell is actually 1 or 2 s later than the load power request. So the φ_k is actually the power request in the $k-1$ time sample. This power request signal is interpreted from the motor controller. u_k is the fuel cell output power to the DC bus. E_{ff} is the battery charging/discharging efficiency, and also should come from real-time signals at battery terminals.

2.5. Cost function analysis

The total cost function to be minimized (J_k) is given by

$$J_k = 0.5P_k[x_N - 0.8C]^2 + 0.5\sum_{k=i}^{N-1}[Q_k(x_k - 0.6C)^2 + R_k {u_k}^2] \tag{8}$$

where P_k, Q_k, R_k are weighting variables, C is the maximum battery capacity, which is fixed (not considering battery depreciation), x_N is the final battery SOC, and x_k is the battery SOC at the kth time interval.

For ICE plug-in hybrid vehicles, it is not necessary to require that the battery SOC recover to almost full after a long driving cycle. This is because the battery stack is quite large and it is supposed to get recharged overnight. The main goal of ICE plug-in vehicles is to decrease pollution by providing longer electric-only range. This concept does not apply here since the fuel cell does not pollute if a reformer is not used. However, because a fuel cell has a relatively low efficiency and requires more maintenance than a battery, it is desirable to use the battery as much as possible, thus the battery final SOC is not limited and still needs to be plugged-in overnight. This is a new concept of a "fuel cell plug-in vehicle".

With this free-final-state control the system is optimally controlled by adding a feedback close-loop controller. Typical fixed-final-state optimal controllers would run open-loop which could be quite unstable [24].

The first term in (8): $(0.5P_k[x_N - 0.8C]^2)$ represents the importance of the final battery state to be close to 0.8 C. If the weighting P is chosen to be very high, then the final state x_N is forced to be very close to 0.8 C, and vice versa. It is understood that this item may not be important if the vehicle designed is a fuel cell plug-in vehicle.

Similarly, the second term in (8): $(0.5\sum_{k=i}^{N-1} Q_k(x_k - 0.6C)^2)$ represents the importance of the battery SOC being kept near 0.6 C for the whole driving cycle. It is typical for the optimum operation of FCEV batteries not to drop the SOC below 40% so as to maintain a long battery life. Additionally, it is also desired not to raise the SOC above 80% to leave some room for capturing any large regenerative braking energy. A larger Q will control SOC to remain close to 60% on the average and keep SOC from changing too rapidly from 40% to 80%.

For the third item in (8): $(0.5\sum_{k=i}^{N-1} R_k {u_k}^2)$ represents the importance of the fuel cell output power magnitude to be limited. A larger R would place more importance on limiting fuel cell output power.

To sum up, first, the system dynamics are given by the physics of the problem (7), while the cost function (8) was chosen to achieve the desired system response. Second, to meet the different control objectives, different weighting variables were assigned and updated in real-time. The different weighting factors in J result in different balances between conforming to the performance objectives and limiting the magnitude of the required optimal controls.

Another item that could be added to the cost function is the fuel cell output power being held close to some percentage of its rated power, such as

$$0.5M_k[u_k - 0.25C_{\text{fuel cell}}]^2$$

where M_k is the importance, and $C_{\text{fuel cell}}$ is the rated fuel cell power. For different fuel cell types, the highest efficiency may vary from 25% to 60% of its peak power. Thus adding this item might be beneficial to the general fuel cell efficiency and the total energy cost. The fuel cell efficiency is more of a dynamic variable considering load change, temperature, pollution, etc., thus this efficiency needs to be tracked in real-time.

Using optimization principles, a sequence of inputs and gains are determined [18,19]. Applying those principles the feedback gain is determined to be

$$K_k = \frac{S_{k+1}\eta E_f}{R_k + S_{k+1}(\eta E_{ff})^2} \tag{9}$$

A feedforward gain is found to be

$$K_k^v = \frac{\eta E_{ff}}{R_k + S_{k+1}(\eta E_{ff})^2} \tag{10}$$

The update series are

$$S_k = \frac{Q_k + S_{k+1}}{1 + (\eta E_{ff})^2 / R_k S_{k+1}} \tag{11}$$

$$v_k = 0.6CQ_k - \left\{ \frac{S_{k+1}((\eta_k E_{ff})^2 v_{k+1}/R_k + \varphi_k Ef)}{(1 + (\eta_k E_{ff})^2 S_{k+1}/R_k) - v_{k+1}} \right\} \tag{12}$$

with the boundary conditions of

$$\begin{aligned} S_N &= P_N \\ v_N &= 0.8CP_N \end{aligned} \tag{13}$$

The fuel cell power command is found to be

$$u_k = \frac{-K_k x_k + K_k^v v_{k+1} - S_{k+1}\varphi_k E_{ff}^2 \eta}{R_k + S_{k+1}(\eta E_{ff})^2} \tag{14}$$

The resultant system equation is

$$x_{k+1} = \frac{(1 - K_k(\eta E_{ff}))x_k + K_k^v(\eta E_{ff})v_{k+1} + \varphi_k E_{ff} R_k}{R_k + S_{k+1}(\eta E_{ff})^2} \tag{15}$$

The different weighting factors in this study were first simulated in US06 highway portion. Fig. 5 shows the battery SOC variation along the driving cycle with an initial 40% charge. In the original cost function, Q represents the importance of battery SOC been held steady. The blue and red curves of Fig. 5 with $Q = 1$ and 1000 show that SOC maintains very close to 60% throughout the cycle, while the green curve with $Q = 0.001$ shows a wide variation of SOC. On the other hand, if $Q = 1$ or 1000 (in Fig. 6), then the fuel cell turns on and off rapidly. Changing P or R with the other variables unchanged can yield similar results showing their individual importance. It is very clear that there is a trade-off between the stability of fuel cell output power and variation in battery SOC or other applicable parameters.

A better battery SOC and fuel cell output power under US06 driving cycle were obtained by assigning the values $R = 40$, $Q = 0.025$ and

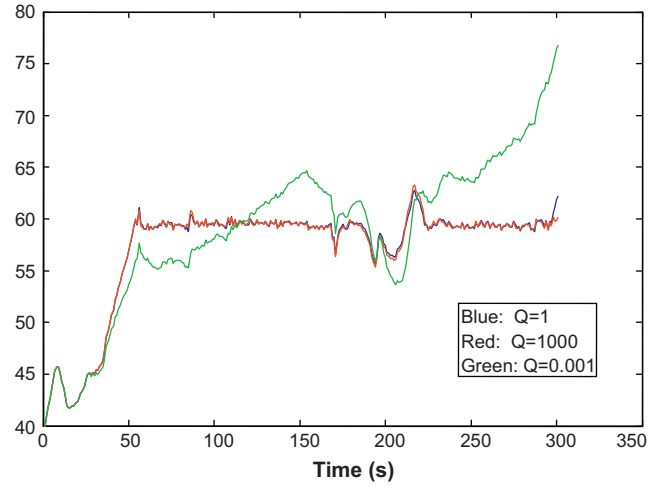

Fig. 5. Battery SOC: $R=P=1$, with various values of Q (blue: $Q=1$, red: $Q=1000$, green: $Q=0.001$). (For interpretation of the references to color in this figure legend, the reader is referred to the web version of the article.)

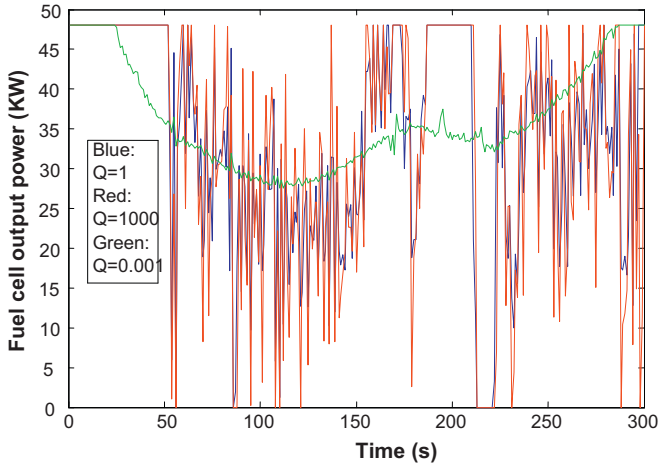

Fig. 6. Fuel cell output power: $R=P=1$, with various values of Q.

$P=1$. The corresponding results are shown in Figs. 7 and 8, respectively. For simplicity, Q is assumed to be inversely proportional to R.

As stated above the problem with optimal control systems in this situation is that diving conditions need to be known in advance to

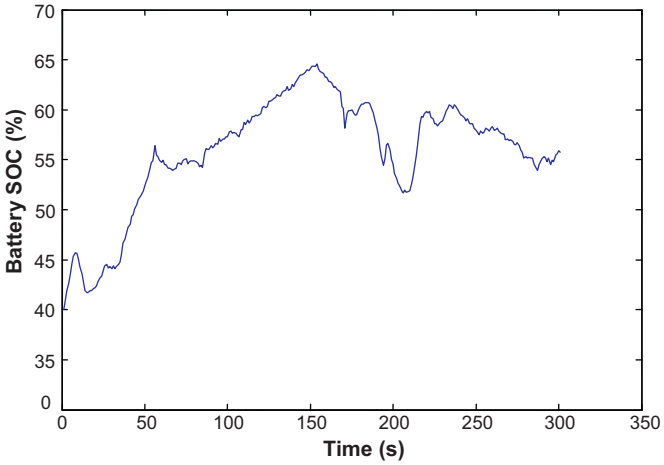

Fig. 7. Battery SOC, $R=40$, $Q=0.025$, $P=1$.

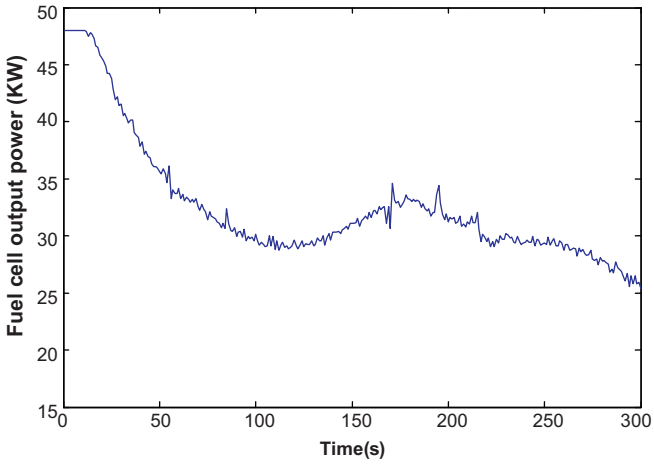

Fig. 8. Fuel cell output power, $R=40$, $Q=0.025$, $P=1$.

determine the optimum path. Therefore an iterative control was developed to determine the control over small time windows.

2.6. Iterative controller

In urban driving cycle where less than average power request is normal, the weighting variable R could be high and the corresponding fuel cell energy cost is limited. However, for a highway driving cycle, R must be low to protect battery from over-discharging since the fuel cell may need to continuously provide peak power. Thus the choices of R and Q only depend on either the average power request or the battery SOC. However, for global optimization like this, the average power required is not predictable, thus the control variables cannot be pre-determined and they can never be changed. Therefore, a period of observing time, the window length (WL), is required to design a feed-back and feed-forward controller.

If the WL is too short (for ICE only vehicle, WL is 0), the fuel cell will go through rapid transients, which must be prevented in order to keep the fuel cell healthy. Alternatively, if it is too long, the batteries may become near depleted before the fuel cell boosts the output power. Thus, it becomes apparent that the optimum WL may change based on the driving cycle. Since highway driving usually has more rapid change in load and higher power requirement, its WL can be used in both urban and highway driving.

When the vehicle is starting, the battery will charge the fuel cell auxiliaries and provide traction power during the first WL. During this time a controller with a previously determined R and Q is used. The vehicle will produce a new R and Q to update the controller for the next WL. Since a vehicle is always started at low speed (urban driving), the weighting coefficients are assigned for urban driving first. If the vehicle is accelerating and needs more power, the battery SOC will fall lower and faster than assumed. Thus, the weighting coefficients will be re-adjusted each step until SOC finally goes up again. If SOC is higher than expected, the coefficients are again adjusted to limit the fuel cell output power. Therefore the controller coefficients can be updated just by observing the battery SOC. This concept is close to fuzzy control, "when if not enough, then add or decrease a bit more".

For every window length, R and Q are updated as:

$$R = R \pm \left|\mathrm{SOC}_{\mathrm{ref}} - \mathrm{SOC}\right| \text{ gain} \times R$$
$$Q = \frac{1}{R} \tag{16}$$

where $\mathrm{SOC}_{\mathrm{ref}}$ is the reference SOC (60%).

The process for updating coefficients is shown in Fig. 9. The gain is also re-adjusted each step, so the control variable update speed

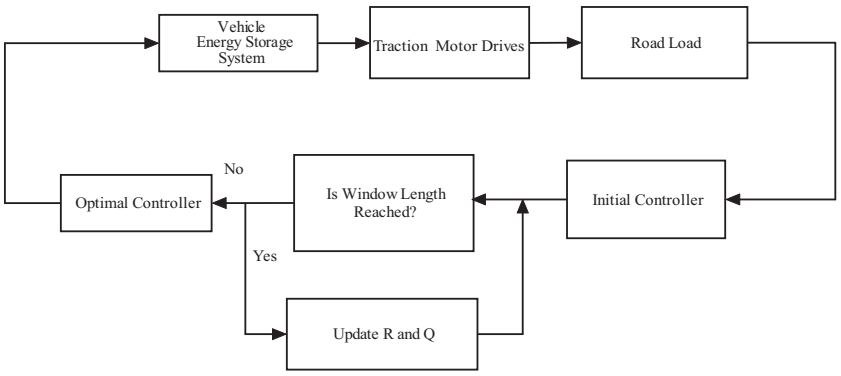

Fig. 9. Update procedures for the *F*/*B* controller.

can always catch up with the battery SOC. Note that the gain is optimized for aforementioned urban and highway driving cycles only; for other cycles with more severe transients, the gain must be increased.

2.7. Optimization of power split for battery/supercapacitor hybrid

Whenever possible, the battery performance is further improved by using a supercapacitor as a power buffer. However, the fuel cell optimal control sequence is independent of the battery/supercapacitor power split since its unidirectional.

The power split between battery and supercapacitor is based on the system

$$x_k\eta_c + y_k\eta_{\text{bat}} = \phi_k \tag{17}$$

where x_k is the supercapacitor input/output power, y_k is the battery input/output power, η_{bat}, η_{cap} is the individual charge/discharge efficiency based on internal resistance change, load current change, etc., ϕ_k is the power requirement over the whole sampling time, which is the difference between the driving cycle load requirement and the fuel cell control input power.

$$\phi_k = \varphi_k - u_k \tag{18}$$

The cost function minimized for this system is

$$J_k = \alpha\sum_{k=i}^{N-1}[(x_k - x_{\max})^2 + (y_k - y_{\max})^2] + \beta\sum_{k=i}^{N-1}(x_k^2) + \gamma\sum_{k=i}^{N-1}(y_k^2) + \delta\sum_{k=i}^{N-1}\left(\frac{\phi_k}{\eta - x_k - y_k}\right)^2 \tag{19}$$

where $\alpha, \beta, \gamma, \delta$ are weighting variables, x_k, y_k are the supercapacitor and battery power at interval k, $x_{\max}$ is the maximum supercapacitor discharge power, $y_{\max}$ is the maximum battery discharge power.

The terms of this cost function are discussed below:

1: $(x_k - x_{\max})^2$ is the importance of the supercapacitor input or output power being limited.
2: $(y_k - y_{\max})^2$ is the importance of the battery's charging or discharging power.
3: $\beta\sum_{k=i}^{N-1}(x_k^2) + \gamma\sum_{k=i}^{N-1}(y_k^2)$ is a weighting function on the total energy cost. If the supercapacitor capacity is low, then weighting β should be enhanced. Similarly γ should be increased for a low battery capacity.
4: $\delta\sum_{k=i}^{N-1}(\phi_k/\eta - x_k - y_k)^2$ is the tolerance of the difference between the power requested and the total power delivered by the battery and supercapacitor.

The controls yet described do not take into account many of the practical requirements for a hybrid vehicle. Additional items included in the implementation of the experimental vehicle control are listed below:

(a) There is additional power required from the battery to drive fuel cell auxiliary systems and other vehicle loads such as headlights, the desired minimum load on the battery is 1 kW. There could be a separate 1 kW DCDC converter which steps down from 300 V to 12 V or 24 V system.
(b) For a supercapacitor, its SOC is given by the energy that can be stored within the capacitor system. The energy stored in supercapacitor is

$$E = 0.5CV^2 \tag{20}$$

Thus

$$\text{SOC} = KV_c{}^2 \tag{21}$$

For the proposed system "*K*" is 1.11×10^{-5}. It yields SOC = 0 for no voltage on the capacitor and SOC = 1 for the maximum voltage of 300 V DC (ideal). For a normal DC–DC converter, its efficiency is assumed to not change much at half the normal input voltage. Here for simplicity, the supercapacitor output voltage is maintained to be higher than 150 V, corresponding to a SOC of 25%. However, during tough transients, this margin is allowed to go down.
(c) For fuel cell, its output power sequence follows the optimal control law. When its power is not required for traction, it is at rest but still operating at a minimum power. This is because restarting the fuel cell takes some time especially at cold weather. The fuel cell is fully turned off only if the key is pulled out.
(d) A power resistor is used to avoid over-charging the battery and super capacitor. When there is incoming regenerative braking energy and either the battery or supercapacitor are both almost fully charged or the re-charge current is above the limit this resistor dissipates the excess power.

For B/C hybrid:

(e) When either the battery or supercapacitor SOC is too low (for battery, the limit is 40%; for supercapacitor, 25%), they will be prevented from giving out power. But if traction power is not enough, they will still be drained.
(f) When either the battery or supercapacitor SOC is too high (for battery, the limit is 90%; for supercapacitor, 100%), they will be forced to deliver power but never absorb any.
(g) If both the battery and supercapacitor SOCs are too low, then they are both protected from discharging, and only the fuel cell gives power. Either battery or supercapacitor has its priority to

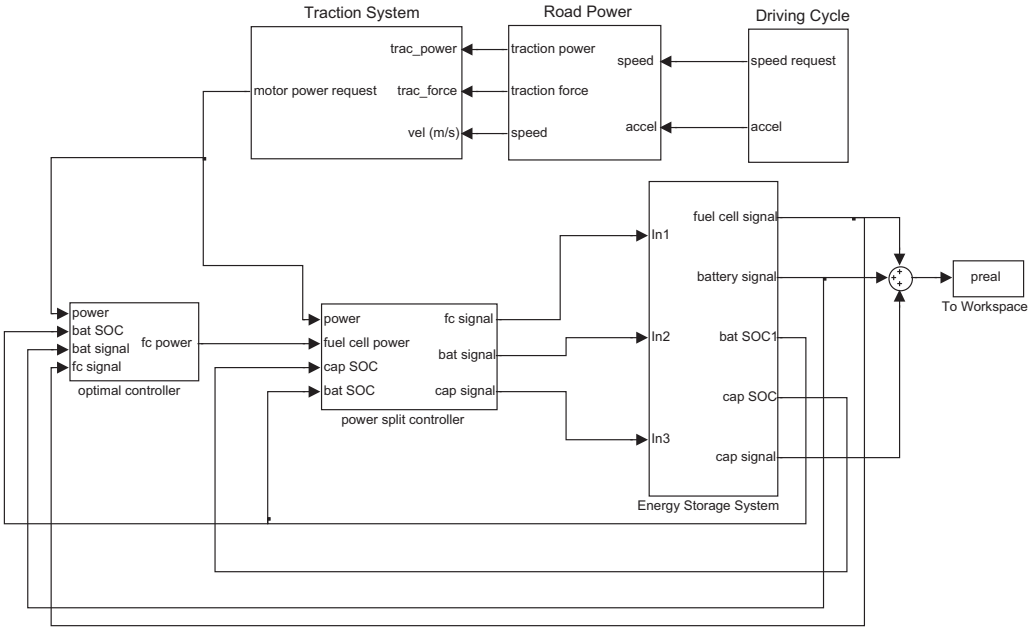

Fig. 10. Simulation model [19].

receive power depending on their individual SOC comparing to reference SOC. If there is higher power demand than the fuel cell can take, either battery or supercapacitor will discharge based on SOC levels.

(h) If both the battery and supercapacitor SOCs are too high, then they are forbidden to get recharged.

(i) If incoming power request is larger than the battery and supercapacitor can handle, then fuel cell should give more power than the optimal results, until it reaches the peak 48 kW limit.

(j) Other than these situations, all components give and receive power in an optimal controlled way.

2.8. Description of simulation model

Fig. 10 shows the simulation model used in the paper. The first block is the duty cycle block that provides speed signals required at the wheel side and also calculates the acceleration. The road power block represents the vehicle model, which calculates the real-time vehicle traction force and power required at the wheel side. The force required comes from overcoming acceleration power, drag power, and rolling resistance. Based on previous traction force and power, and the transmission gear ratio, the motor block calculates real power cost at the power system end from a motor efficiency lookup table.

The fourth block is the optimal controller output. It receives the power command and attempts to force the fuel cell and battery hybrid to follow the optimal power flow sequence. It also receives feedback signals as battery power cost, fuel cell power cost, and real time battery SOC. The fifth block is the system (power split) controller; it forces battery and supercapacitor to follow the optimal control flow if possible, then provides all system protection features enumerated in Section 2.7. It receives real time supercapacitor SOC and battery SOC feedback. The sixth block is the energy storage system block, which is a simulation of each individual system's efficiency versus power request. The outputs are summed into a real power cost.

3. Results and discussion

To compare the new proposed optimal control strategy, a thermostatic control strategy (otherwise called charge depletion mode) was studied first. Here the fuel cell is turned on at its peak output power when battery SOC falls down below 40%, and is turned off when battery SOC has recovered to 80%. The battery/supercapacitor hybrid follows the same optimal controlled method.

Fig. 11 indicates highway driving for 5 h. It seems that for thermostatic strategy, the fuel cell is near always turned on at maximum 48 kW except for some brief intervals where it just shut down. However, the fuel cell is never turned-off for optimal strategy and gives out 10–48 kW. The battery SOC is maintained slightly closer to its desired value for optimal strategy.

However, the optimal strategy appears to be working much better under urban driving. Instead of frequently turning on and off, the fuel cell only needs to be kept running at about 5–15 kW and never turns off. The battery SOC is also much better, being kept about 50–70% (Fig. 12).

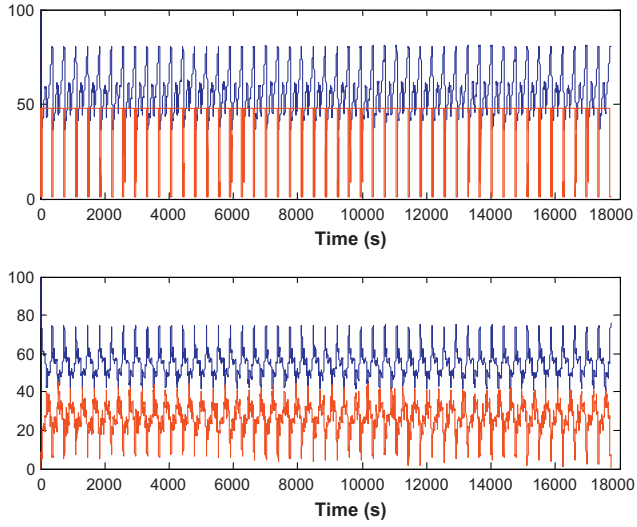

Fig. 11. Battery %SOC (blue) and fuel-cell output power (kW) (red) for US06 highway cycle. Top: thermostatic design. Bottom: optimal design. (For interpretation of the references to color in this figure legend, the reader is referred to the web version of the article.)

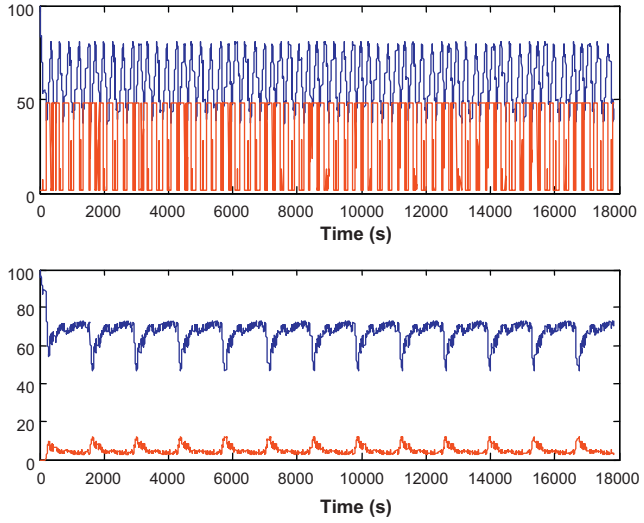

Fig. 12. Battery %SOC (blue) and fuel-cell output power (kW) (red) for UDDS urban cycle. Top: thermostatic design. Bottom: optimal design. (For interpretation of the references to color in this figure legend, the reader is referred to the web version of the article.)

The difference in the optimal control performance between the highway and urban driving cycle is due to the limited size of the fuel cell, it cannot always provide the optimal calculated result during highway driving, but is forced to provide its peak power to prevent battery from depleted.

The battery performance throughout a short US06 driving cycle is shown in Fig. 13. The top panel is the required output or input power at the battery side, the middle panel shows the real power cost of the battery due to efficiency, the bottom panel shows the variation of battery SOC.

Fig. 14 shows the supercapacitor SOC and power output during a short US06 driving cycle.

Another interesting situation that may occur with a plug-in type vehicle is when the battery is not pre-charged and when the customer starts up a vehicle with no time to wait. The worst case is

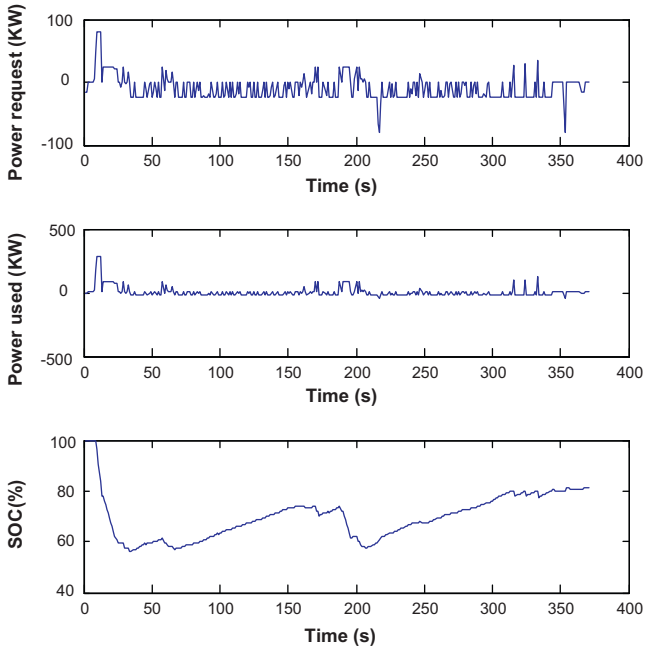

Fig. 13. Battery performance for US06 driving cycle.

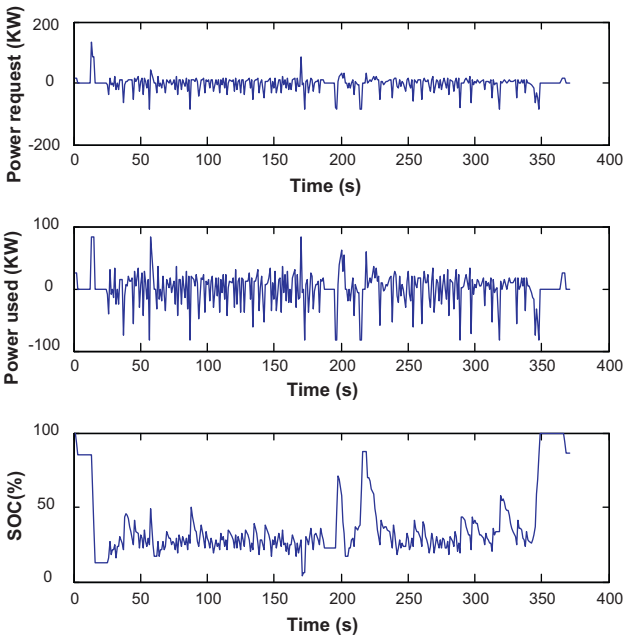

Fig. 14. Supercapacitor performance for US06 driving cycle.

when the battery initial SOC is only 40% at the beginning (remember the battery is forbidden to discharge below this point), and there is a rapid motor power request within the first 10 s. Here the optimal controller ensures that the fuel cell will be turned on for a longer time, and the battery will only face a little more loss in efficiency (or battery life). The battery will be gradually re-charged during the driving process as shown in Fig. 15.

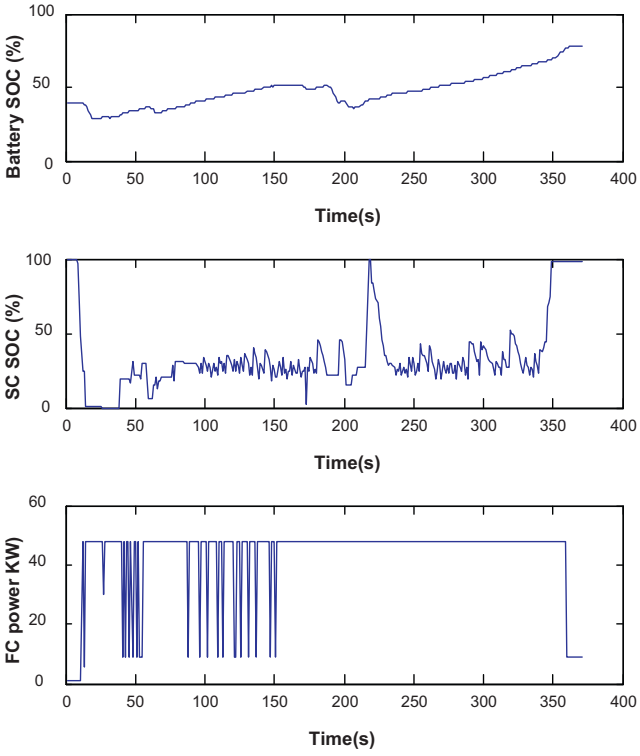

Fig. 15. Performance for a non-precharged fuel cell plug-in vehicle. Top panel: battery SOC. Middle panel: supercapacitor SOC. Bottom panel: fuel cell power output.

Table 3
Driving cycle comparison based on simulated result.

	City driving	Highway driving	Long city	Long highway
Time (s)	1370	369	16,440	17,712
Distance (km)	11.99	10.04	143.88	481.72
Average speed (km h^{-1})	31.51	97.91	31.51	97.91
Maximum speed (km h^{-1})	91.2	129.2	91.2	129.2
Average traction power (kW)	3.21	18.28	3.21	18.28
Maximum traction power (kW)	75.05	197.6	75.05	197.6
Maximum braking power (kW)	58.82	148.8	58.82	148.8
Energy cost (kWh) thermostatic	5.67	4.68	73.71	224.64
Energy cost (kWh) optimal	3.05	4.37	39.65	209.76

Table 3 summarizes the simulation results for both the thermostatic and optimal control. Several standard driving cycles were used in this comparison.

From Table 3, it is seen that when compared to the thermostatic control, the described optimal control saves 46.21% of the energy required in long city driving cycle and 6.62% of the energy required in highway driving cycle. In the latter application, the fuel cell is frequently turned on at full power (saturated result), thus optimal results are seldom reached. It is anticipated that with a larger fuel cell, the efficiency can be further increased. Moreover, since battery SOC is strictly monitored and controlled to remain around 60%, battery life will be increased.

4. Conclusion

This paper proposed a dynamic power distribution among a three-component hybrid system. The F/B and B/C hybrids are individually optimal controlled, and a global optimization controller with real time capability is proposed. Simulations show that the proposed optimal control is better than common thermostatic controls. Not only does it keep the devices working closer to their optimal operating points, but it also shows considerable energy saving over several different driving cycles.

Acknowledgements

Funding of this research in part by the Department of Transportation is gratefully acknowledged.

References

[1] M.J. Ogburn, Systems integration, modeling, and validation of a fuel cell hybrid electric vehicle, Master's thesis in Mechanical Engineering, Virginia Polytechnic Institute and State University, 2000.
[2] H. Zhao, A.F. Burke, EVS24 International Battery, Hybrid and Fuel Cell Electric Vehicle Symposium, Stavanger, Norway, 2009.
[3] Z. Jiang, L. Gao, M.J. Blackwelder, R.A. Dougal, Journal of Power Sources 130 (2004) 163–171.
[4] P. Thounthong, S. Raël, B. Davat, I. Sadli, IEEE-PESC06, 2006, pp. 1991–1997.
[5] P. Rodatz, G. Paganelli, A. Sciarretta, L. Guzzalla, Control Engineering Practice IS/13/1 (2005) 41–53.
[6] P. Thounthong, S. Rael, B. Davat, IEEE-APEC2005, 2005, pp. 90–96.
[7] J. Moreno, M. Ortúzar, J. Dixon, IEEE Transactions on Industrial Electronics 53 (2006) 614–623.
[8] W. Gao, IEEE Transactions on Vehicular Technology 54 (2005) 846–855.
[9] B. Yuwen, D. Zhu, X. Jiang, Proceedings of International Conference on Power System Technology, vol. 1, 2002, pp. 149–152.
[10] A. Drolia, P. Jose, N. Mohan, IEEE-IECON03, vol. 1, 2003, pp. 897–901.
[11] P. Thounthong, P. Sethakul, S. Rael, B. Davat, IEEE-IAS2009, 2009, pp. 1–8.
[12] R.M. Schupbach, J.C. Balda, IEEE-PESC04, vol. 3, 2004, pp. 2157–2163.
[13] S.S. Willamson, S. Lukic, A. Emadi, IEEE Transactions on Power Electronics 21 (2006) 730–740.
[14] M.B. Camara, H. Gualous, F. Gustin, A. Berthon, IEEE Transactions on Vehicle Technology 57 (5) (2008) 2721–2735.
[15] F.H. Khan, L.M. Tolbert, IEEE-IAS2007, 2007, pp. 628–635.
[16] J.L. Duarte, M. Hendrix, M. Godoy Simões, IEEE Transactions on Power Electronics 22 (2007) 480–487.
[17] D. Liu, H. Li, IEEE Transactions on Power Electronics 21 (2006) 1513–1517.
[18] Z. Yu, Static and dynamic optimal controls for fuel-cell hybrid vehicle power system, Master's thesis in Electrical Engineering, Northern Illinois University, 2007.
[19] A. Bose, D. Zinger, Z. Yu, Active electrical power flow control system for optimization of power delivery in electric hybrid vehicles, Patent application No: #12/137,849 (2008).
[20] AC55 Motor Product Specifications, Azure Dynamics, http://www.azuredynamics.com/products/force-drive/documents/AC55_DMOC445ProductSheet.pdf.
[21] J.M. Mucha, System control strategies for a series hybrid electric vehicle, Master thesis in Mechanical Engineering, University of Illinois at Urbana-Champaign, 2001.
[22] L. Lu, M. Liu, M. Ouyang, Journal of Asian Electric Vehicles 2 (2004) 1–5.
[23] S. Delprat, T.M. Guerra, G. Paganelli, J. Lauber, M. Delhom, Proceedings of American Control Conference 2 (2001) 1315–1320.
[24] F.L. Lewis, V.L. Syrmos, Optimal Control, John Wiley & Sons, 1995.
[25] ADVISOR 2.0, http://www.nrel.gov/vehiclesandfuels/vsa/pdfs/25928.pdf.